Applied Mathematical Sciences, Vol. 8, 2014, no. 33, 1605 - 1620
HIKARI Ltd, www.m-hikari.com
http://dx.doi.org/10.12988/ams.2014.4138

On the Finite-Element-Based Lattice Boltzmann Scheme

G. V. Krivovichev

Department of Applied Mathematics and Processes of Control
Saint-Petersburg State University, Saint-Petersburg
Russian Federation

Abstract

The finite-element-based lattice Boltzmann scheme for the computations on unstructured meshes is proposed. The scheme is based on the weighted residuals method with Galerkin approximation. The scheme is reduced to the solution of the linear algebraic system at every time step. The possibilities of application of the developed scheme for practical problems are demonstrated on the applications to two test problems of computational fluid dynamics. The investigation of the equilibrium boundary conditions for distribution functions is performed. The obtained results demonstrate that this type of boundary conditions can produced a results which are in good agreement with the results obtained from the solution of hydrodynamical equations at $Re \geq 20$. The algorithm of the proposed scheme is realized in GNU license software `freefem++ v.3.20`.

Mathematics Subject Classification: 76-04; 76M10; 65N30

Keywords: lattice Boltzmann method, finite element method, freefem++

1 Introduction

Nowadays the lattice Boltzmann method (LBM) has established itself as a powerful tool for the modelling of a wide range of physical processes. One of its main application is the computational fluid dynamics (CFD), where it has proven successful to solve problems for weakly compressible viscous flows [4], [45] and much more complex situations such as multiphase and multicomponent flows [19], [20], [26], [35], flows in porous media [27] and flows with free surface [33], [52]. The popularity of the method is based on its straightforward parallelism, due to the explicit nature of its numerical scheme with intensive local computation. The method is successfully adopted for computations on single and multiple graphical processing units (GPU) using Compute Unified Device Architecture (CUDA) [32], [33], [49].

The drawback of the traditional form of LBM is that it is constructed to a special class of uniform and regular structured meshes [4], [45]. This factor is limited numerical efficiency of LBM in situations, when there is a need for a high resolution grid in the complex form pattern of for the flow near a curved solid body. As an examples of such problems, the blood flow in real geometries [44],[51], or flows in porous media [27] can be mentioned.

In order to improve numerical efficiency and accuracy of LBM for applications to flows in complex domains, methods with unstructured meshes based on so-called lattice Boltzmann schemes (LBS) have been developed. This type of schemes is based on space discretization of the system of partial differential kinetic equations, obtained from the Bhatnagar — Gross — Krook (BGK) kinetic equation [2] using Broadwell's discrete velocities method [3].

In this study, a new LBS is developed for computations of viscous flows using unstructured meshes. The scheme is based on the finite element discretization using Galerkin approximation. The possibilities of application of the developed scheme for practical problems are demonstrated on the applications to two test problems of CFD. The algorithm of the proposed scheme is realized in GNU license software `freefem++ v.3.20` [13].

The paper is organized as follows. In Section 2, the lattice Boltzmann equation (LBE) and LBS are discussed. In Section 3, a new finite-element-based scheme is discussed. In Section 4, two test problems of the lid-driven cavity and flow past a circular cylinder are considered and numerical results are discussed. Concluding remarks are made in Section 5.

2 Lattice Boltzmann equation and lattice Boltzmann schemes

In LBM the fluid is represented by an ensemble of mesoscopic particles that move on a regular spatial lattice and undergo collisions at its nodes. Velocities of the particles are formed a discrete set of vectors $\mathbf{V}_i = V\mathbf{v}_i$, $i = 1, \dots, n$, where $V = l/\delta t$ is a typical velocity, δt is a time step, l is a lattice spacing (spatial step). In this paper only planar flows without body force action are considered and a so-called D2Q9 lattice is used. This type of lattice is defined by the following vectors:

$$\mathbf{v}_1 = (0,0), \quad \mathbf{v}_2 = (1,0), \quad \mathbf{v}_3 = (0,1), \quad \mathbf{v}_4 = (-1,0), \quad \mathbf{v}_5 = (0,-1),$$

$$\mathbf{v}_6 = (1,1), \quad \mathbf{v}_7 = (-1,1), \quad \mathbf{v}_8 = (-1,-1), \quad \mathbf{v}_9 = (1,-1).$$

The particle distribution functions f_i are used as main variables. The system of LBE evolution equations with the BGK single relaxation time collision operator is written as:

$$f_i(t_j + \delta t, \mathbf{r}_{kl} + \mathbf{V}_i \delta t) - f_i(t_j, \mathbf{r}_{kl}) = -\frac{1}{\tau}\left(f_i(t_j, \mathbf{r}_{kl}) - f_i^{(eq)}(t_j, \mathbf{r}_{kl})\right), \qquad (1)$$

where $\mathbf{r}_{kl} = (x_k, y_l)$ — is a lattice node, t_j — is a node of the time grid constructed with step δt, $\tau = \lambda/\delta t$ is a dimensionless relaxation time, λ is a real relaxation time, $f_i^{(eq)}$ are the equilibrium distribution functions.

System of finite-difference equations (1) could be derived by different ways — as a special type of lattice gas cellular automata [45] or by discretization of continuous BGK equation [1],[16]. At first stage of the discretization process BGK equation is dicretized in velocity space by Broadwell's discrete velocities method [3]. After this procedure BGK equation is reduced to the system of partial differential equations [1]:

$$\frac{\partial f_i}{\partial t} + V_{ix}\frac{\partial f_i}{\partial x} + V_{iy}\frac{\partial f_i}{\partial y} = -\frac{1}{\lambda}\left(f_i - f_i^{(eq)}\right), \qquad (2)$$

and on the next stages discretisation in time and space is performed.

The fluid density ρ and the velocity $\mathbf{u}$ at a lattice node are calculated as:

$$\rho(t_j, \mathbf{r}_{kl}) = \sum_{i=1}^{9} f_i(t_j, \mathbf{r}_{kl}), \quad \rho(t_j, \mathbf{r}_{kl})\mathbf{u}(t_j, \mathbf{r}_{kl}) = \sum_{i=1}^{9} \mathbf{V}_i f_i(t_j, \mathbf{r}_{kl}). \qquad (3)$$

In applications of LBM to the incompressible viscous fluid flows modelling, the case of the small values of Mach number $M = |\mathbf{u}|/V$ is considered. In this case the expressions for $f_i^{(eq)}$ can be written as [45]:

$$f_i^{(eq)} = W_i \rho \left(1 + 3\frac{(\mathbf{V}_i \cdot \mathbf{u})}{V^2} + \frac{9}{2}\frac{(\mathbf{V}_i \cdot \mathbf{u})^2}{V^4} - \frac{3}{2}\frac{\mathbf{u}^2}{V^2}\right), \qquad (4)$$

where $W_i = 4/9$ for $i = 1$; $1/9$, for $i = 2,3,4,5$; $1/36$, for $i = 6,7,8,9$.

The expression for the kinematic viscosity ν could be derived from the system (2) by application of the Chapman — Enskog method. In the case of D2Q9 lattice, expression for ν can be written as [36],[37]:

$$\nu = \frac{\lambda}{3} V^2. \qquad (5)$$

The computations based on the solution of LBE (1) could be realized only on the lattice, which can be characterized as a structured mesh with regular grid. As it is mentioned above, for some practical problems this factor could be a limitation for the effective usage of LBM.

There are several ways for the avoiding of this limitation. First group of papers is dedicated to special grid refinement and adaptation algorithms based on the solution of LBE (1). In papers of O. Filippova and D. Hanel [8], [9], [10] and S. Foroughi et al [12] a grid-refinement extensions of LBM are developed. These extensions are based on the usage of block-structured grids, which are defined *a priori*. In papers of B. Crouse et al [5], G. Eitel-Amor et al [7] and J. Wu, C. Shu [46] an algorithms of grid adaptation are developed. The local grid resolution is determined during runtime by using local error estimators or heuristic error indicators. These estimators and indicators use the conditions and expressions for macrovariables ρ and $\mathbf{u}$, such as incompressibility condition [5] and absolute values of vorticity [7].

Another group of papers deal with the LBE formulations for curvilinear structured meshes. R. Mei and W. Shyy proposed LBE in orthogonal curvilinear coordinates [23]. M. Mirsaci and A. Poozech proposed a method for LBM computations based on the usage of conformal maps [24].

Some papers are dedicated to the LBS, constructed by the discretization of system (2) by finite difference method (FDM), finite volume method (FVM) or finite element method (FEM). For this type of schemes the unstructured meshes, which are not connected with the lattice, could be used. In [28] these schemes are called *off-lattice* schemes, which mean that mesh is decoupled from the lattice structure and conforms the complex geometry.

The major amount of schemes constructed by FDM are used structured meshes, so the main attention will be focused on the schemes constructed by FVM and FEM.

In papers [28], [29], [30], [39], [40], [41], [47], [48], [50] the LBS's constructed by FVM are proposed. The different approaches to the numerical flux calculation on the boundaries of finite volumes are used. The time derivative of f_i in (2) is approximated with the first order by the right finite difference [29], [30], [41], [47], [48] or with third and fourth order by Runge — Kutta method [28], [50]. In [39] FVM is used for the construction of stable scheme for the parabolic approximation of system (2). It must be noted, that this scheme is constructed not for the system of hyperbolic equations (2), but for the parabolic system, which is constructed using Taylor expansions on space variables.

In [22], [34], [43] LBS's, based on the discretization by FEM, were proposed. The method of weighted residuals with Galerkin approximation is used for scheme construction. The only drawback of its application to hyperbolic systems such as (2) consists with the construction of explicit stable schemes [17]. There are some different approaches to stabilization of this type of schemes

[17]. One approach is based on the reduction of first order hyperbolic system (2) to the system of second order parabolic equations by addiction of specially constructed dissipation terms or by using Taylor expansions. These methods are applied in [22], [34], [43]. It must be noted, that by this approach the numerical scheme is constructed not for the initial system (2), but for the modified system of second order equations. According to this fact, some errors, which are unavoidable, can be produced in numerical solution.

The presented paper is dedicated to the construction of LBS based on FEM discretization. The scheme, which can be classified as semi-implicit, is reduced to the solution of linear algebraic system at every time step. The scheme is based on the initial system (2) and its construction not deal with the reduction to the system of second order equations.

3 Finite-element-based lattice Boltzmann scheme

It is proposed, that initial-boundary problem for the system (2) is stated in domain $\Omega \subset \mathbf{R}^2$. After the triangulation of Ω on M finite elements (triangles) ω_s, $s = \overline{1, M}$, the unstructured mesh with N grid nodes is constructed. Let us define the system of interpolation functions for every node of finite elements $\varphi_j(\mathbf{r})$, $j = \overline{1, N}$. The variables f_i are expressed by the linear combinations:

$$f_i(t, \mathbf{r}) = \sum_{j=1}^{N} F_i^j(t)\varphi_j(\mathbf{r}),$$

where the variables $F_i^j(t)$ must be defined. The last expression can be written in vector form:

$$f_i(t, \mathbf{r}) = \mathbf{F}_i^T(t)\mathbf{\Phi}(\mathbf{r}), \tag{6}$$

where $\mathbf{F}_i = (F_i^1, \ldots, F_i^N)^T$, $\mathbf{\Phi} = (\varphi_1, \ldots, \varphi_N)^T$.

After the substitution of (6) in (2) it can be written:

$$\dot{\mathbf{F}}_i^T(t)\mathbf{\Phi}(\mathbf{r}) + \mathbf{V}_i(\nabla\mathbf{\Phi}(\mathbf{r}))^T\mathbf{F}_i(t) =$$

$$= -\frac{1}{\lambda}\Big(\mathbf{F}_i^T(t)\mathbf{\Phi}(\mathbf{r}) - f_i^{(eq)}(\mathbf{F}_1(t), \ldots, \mathbf{F}_9(t), \mathbf{\Phi}(\mathbf{r}))\Big), \tag{7}$$

where $\dim(\nabla\mathbf{\Phi}) = N \times 2$.

According to the standard procedure of the weighted residuals method with Galerkin approximation [11], [18], let us compute (7) for every i on $\mathbf{\Phi}$ and integrate over the whole domain Ω:

$$\sum_{s=1}^{M} \int_{\omega_s} \Big(\dot{\mathbf{F}}_i^T(t)\mathbf{\Phi}(\mathbf{r}) + \mathbf{V}_i(\nabla\mathbf{\Phi}(\mathbf{r}))^T\mathbf{F}_i(t)\Big)\, \mathbf{\Phi}(\mathbf{r})d\mathbf{r} =$$

$$= -\frac{1}{\lambda}\sum_{s=1}^{M}\int_{\omega_s}\left(\mathbf{F}_i^T(t)\mathbf{\Phi}(\mathbf{r}) - f_i^{(eq)}(\mathbf{F}_1(t),\ldots,\mathbf{F}_9(t),\mathbf{\Phi}(\mathbf{r}))\right)\mathbf{\Phi}(\mathbf{r})d\mathbf{r}, \quad (8)$$

where $d\mathbf{r} = dxdy$.

From (8) the system of ordinary differential equations for $\mathbf{F}_i(t)$ can be obtained:

$$\mathbf{A}\dot{\mathbf{F}}_i(t) + \mathbf{B}_i\mathbf{F}_i(t) = -\frac{1}{\lambda}\left(\mathbf{A}\mathbf{F}_i(t) - \mathbf{G}_i(\mathbf{F}_1(t),\ldots,\mathbf{F}_9(t))\right), \quad (9)$$

where

$$\mathbf{A} = \sum_{s=1}^{M}\int_{\omega_s}\mathbf{\Phi}(\mathbf{r})\mathbf{\Phi}^T(\mathbf{r})d\mathbf{r}, \quad \mathbf{B}_i = \sum_{s=1}^{M}\int_{\omega_s}\mathbf{\Phi}(\mathbf{r})\mathbf{V}_i(\nabla\mathbf{\Phi}(\mathbf{r}))^T d\mathbf{r},$$

$\mathbf{G}_i \in \mathbf{R}^N$ are nonlinear vector-functions.

For the time approximation of (9) the single-step implicit approximation of $\dot{\mathbf{F}}_i(t)$ at node $t = t_{j+1}$ is used:

$$\mathbf{A}\left(\frac{\mathbf{F}_i(t_{j+1}) - \mathbf{F}_i(t_j)}{\Delta t}\right) + \mathbf{B}_i\mathbf{F}_i(t_{j+1}) =$$

$$= -\frac{1}{\lambda}\left(\mathbf{A}\mathbf{F}_i(t_{j+1}) - \mathbf{G}_i(\mathbf{F}_1(t_{j+1}),\ldots,\mathbf{F}_9(t_{j+1}))\right), \quad (10)$$

where Δt is the time step. In general $\Delta t \neq \delta t$.

For the computation of $\mathbf{F}_i(t_{j+1})$ from (10) the system of nonlinear algebraic equations must be solved. For the simplification of solution process the nonlinear term can be compute on the previous time step by the formulae:

$$\mathbf{G}_i(\mathbf{F}_1(t_{j+1}),\ldots,\mathbf{F}_9(t_{j+1})) \approx \mathbf{G}_i(\mathbf{F}_1(t_j),\ldots,\mathbf{F}_9(t_j)), \quad (11)$$

which give first order approximation of $\mathbf{G}_i$ in $t = t_{j+1}$.

After the substitution of (11) into (10), the finite difference scheme is constructed:

$$\mathbf{A}\left(\frac{\mathbf{F}_i(t_{j+1}) - \mathbf{F}_i(t_j)}{\Delta t}\right) + \mathbf{B}_i\mathbf{F}_i(t_{j+1}) =$$

$$= -\frac{1}{\lambda}\left(\mathbf{A}\mathbf{F}_i(t_{j+1}) - \mathbf{G}_i(\mathbf{F}_1(t_j),\ldots,\mathbf{F}_9(t_j))\right),$$

the last expression can be written in following form:

$$\left(\left(1 + \frac{\Delta t}{\lambda}\right)\mathbf{A} + \Delta t\mathbf{B}_i\right)\mathbf{F}_i(t_{j+1}) =$$

$$= \mathbf{A}\mathbf{F}_i(t_j) + \frac{\Delta t}{\lambda}\mathbf{G}_i(\mathbf{F}_1(t_j),\ldots,\mathbf{F}_9(t_j)). \quad (12)$$

It can be seen, that the usage of (12) consists with the solution of linear algebraic system at every time step.

The developed scheme is applied to the numerical solution of CFD test problems, such as lid-driven cavity flow (the case of straight boundaries) and to the flow past a circular cylinder (the case of curvilinear boundaries). Obtained results showed a good agreement with the results, obtained from the solution of hydrodynamical equations.

4 Numerical solution of the test problems

Program realization of the algorithm of proposed scheme was performed in `freefem++ v.3.20` [13], which have all possibilities to realization of FEM application to practical problems.

The linear interpolation functions $\varphi_j(\mathbf{r})$ are used. The computation of integrals is performed by Simpson's quadrature rule.

One of the main problems of LBM consist with the fact, that boundary conditions (BC) have to be imposed to the distribution functions f_i rather than on hydrodynamical variables such as density, velocity, pressure and stress tensor. At the same time, BC for physical problems are formulated for the hydrodynamical variables. There are several ways of incorporation of the hydrodynamical conditions to the conditions for f_i with different orders of accuracy and various characteristics on stability [21], [42].

In the presented paper one of the simplest types of BC, called equilibrium boundary condition (EBC) is used. This type consist with the proposition, that boundary values of f_i are equal to the values of $f_i^{(eq)}$, which can be calculated by (4) from the boundary values of ρ and $\mathbf{u}$. The EBC can be realized without any troubles for the boundaries with arbitrary curvilinear geometric form, in contrast to bounce-back BC, which needs some special modifications for the case of complex boundaries, where the interpolation can be problematic and error-prone [25], [31], [39].

There are some physical restrictions on the application of EBC to hydrodynamical problems. This type of BC can be applied only in a regime of low wall-shear flow, because in EBC shear stress near the wall is neglected [25]. A. Mohamad and S. Succi in [25] showed that the usage of EBC for the problem of backward facing-step flow at Reynolds number $Re \approx 500$ can produced accurate results in comparison with the case of nonequilibrium BC, which take into account existence of shear stress near the wall.

In the presented paper the investigation of the EBC application in cases of $Re \in [10, 100]$ is realized. The effect of EBC on the accuracy of numerical results is demonstrated for two test problems.

The main input parameter of the program is Re, which is calculated as:

$$Re = \frac{UL}{\nu}, \tag{13}$$

where L is typical length, U is typical velocity. Parameters U and L are inputted before the computation. Kinematic viscosity ν is calculated by (13) from the values of Re, L and U. Parameter λ is calculated from the value of ν by formulae (5).

The values of l and δt are chosen to be equal. The values of f_i at the initial moment $t = 0$ are assumed to be equal to the values of $f_i^{(eq)}$. The velocity $\mathbf{u}$ at this moment is chosen as zero vector at all grid points and the initial density is chosen to be equal to unity.

4.1. Lid-driven cavity flow. In case of this problem Ω is presented as: $\Omega = \{(x, y)|x \in [0, P], y \in [0, P], P > 0\}$. The boundary conditions has a form:

$$u_x(t, x, 0) = u_y(t, x, 0) = 0, \quad u_x(t, x, P) = U_0, u_y(t, x, P) = 0, \quad x \in [0, P],$$

$$u_x(t, 0, y) = u_y(t, 0, y) = u_x(t, P, y) = u_y(t, P, y) = 0, \quad y \in [0, P),$$

where $U_0 = const \neq 0$ is the velocity of the top lid. For the Re computation in (13) it can be proposed that $U = U_0$ and $L = P$. The following values of the parameters are used: $P = 1$ m, $U_0 = 0.1$ m/s. The time interval from 0 to 400 s is considered. Time grid with $2 \cdot 10^5$ nodes is used. The unstructured mesh with 5854 triangles and 3028 nodes is used (fig. 1).

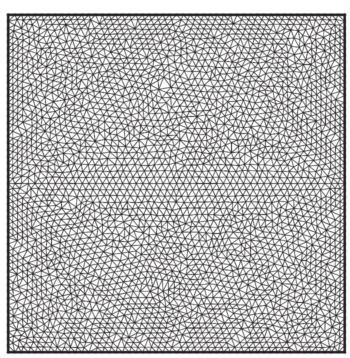

Fig. 1. Unstructured mesh for the lid-driven cavity flow problem

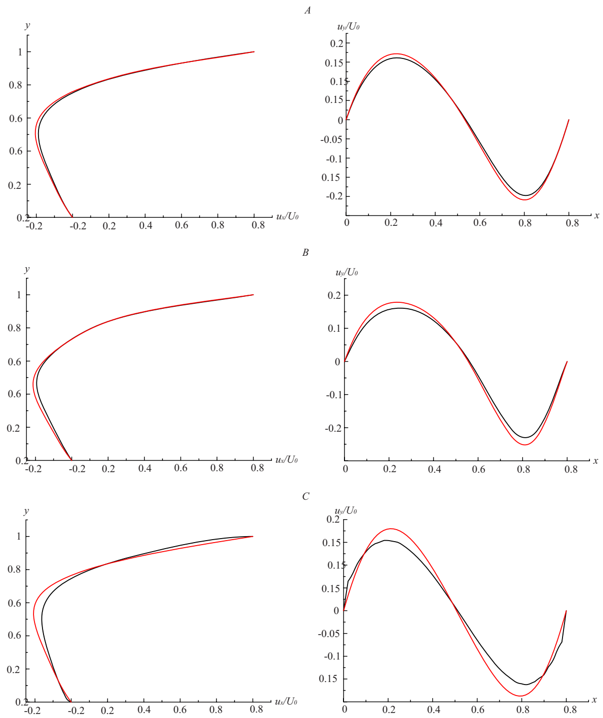

Fig. 2. Plots of the velocity components for lid-driven cavity flow. Black line corresponds to the solution obtained by LBS, red line — to the solution obtained from hydrodynamical equations. A — case of $Re = 50$, B — case of $Re = 100$, C — case of $Re = 10$.

Numerical results, obtained by LBS are compared with the results, obtained after the solution of hydrodynamical equations in "vorticity — stream functions" variables. The criterion for the comparison is calculated by the following formulae:

$$I = \sqrt{I_x^2 + I_y^2},$$

where I_x and I_y are calculated as:

$$I_x = \frac{1}{N}\sum_{i=1}^{N}\left(u_x(T, 0.5P, y_i) - U_x(T, 0.5P, y_i)\right)^2,$$

$$I_y = \frac{1}{N}\sum_{i=1}^{N}\left(u_y(T, x_i, 0.5P) - U_y(T, x_i, 0.5P)\right)^2,$$

where T is the length of time interval; U_x, U_y — velocity components, obtained after the hydrodynamical equations solution; $N = 100$ is the number of the nodes of the grid, constructed in space interval $[0, P]$.

The values of I are presented in Table 1 for different values of Re. As it can be seen, the value of I is decreased until the value of Re is tend to 80. It is the typical situation, because with the increasing of Re the influence of the viscosity as the influence of the shear stress became weak and not essential. The increasing of the values of I after the rising of Re from 80 can be explained by the formation of vorticity near the right wall, which is correspond to the value of $x = P$ [14]. The vorticity formation tend to the increasing of shear stress values.

Table 1. The values of I at different Re values for lid-driven cavity flow.

Re	10	20	30	40	50	60	70	80	90	100
$I \cdot 10^4$	17.1	4.65	2.38	1.62	1.31	1.16	1.12	1.20	1.50	2.04

The plots of u_x/U_0 and u_y/U_0 at $Re = 50$, 100 and 10 are presented in fig. 2. The plots of u_x/U_0 are presented at the points of the line $\{x = 0.5P, y \in [0, P]\}$, plots of u_y/U_0 — at the points of the line $\{x \in [0, P], y = 0.5P\}$. As it can be seen from fig. 2 C, in the case of $Re = 10$ there are some deviations of the values of LBS solution from the values of U_x and U_y. These deviations can be explained by the fact, that in the case of $Re = 10$ the influence of the shear stress is essential and can not be ignored.

4.2. Planar flow past a circular cylinder. The statement of the problem is presented in [6], [23]. The flow between two cylinders of radii r_0 and R is considered. On the cylinder with radius r_0 the components of $\mathbf{u}$ are proposed equal to zeros, on the cylinder with radius R the following values are stated: $u_x = U_0 \neq 0, u_y = 0$. For the Re computation from (13) it is proposed that $U = U_0$, $L = 2r_0$.

The following parameters values are used: $r_0 = 0.05$ m, $R = 0.5$ m, $U_0 = 0.01$ m/s. The time interval from 0 to 2000 s is considered with the time grid with 10^5 nodes. The unstructured mesh contained 5608 triangles and 2889 grid nodes is used (fig. 3).

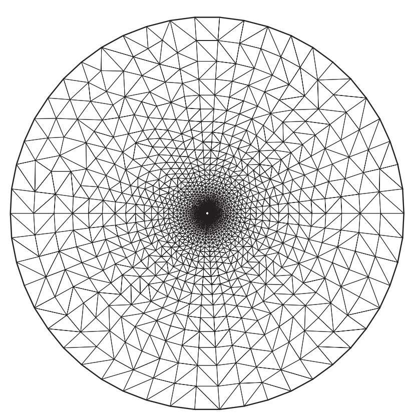

Fig. 3. Unstructured mesh for the flow past a circular cylinder

As the results of computations the values of dimensionless drag coefficient $C_D = (1/(\rho r_0 U_0^2)) \int_D S_{x\alpha} n_\alpha ds$ (where D — is the circle with radius r_0; n_x, n_y components of the normal to D; S_{xx}, S_{xy} are the components of stress tensor) are obtained.

As it is known (see [38]), for the case of the flow over circular cylinder, the flow is became stationary until $Re < Re_c \approx 50$, with two symmetric vortices over the cylinder. After Re_c the flow became periodic in time with the development of von Karman vortices over the cylinder.

In the presented paper the calculations of C_D values are realized only for the cases of $Re < Re_c$. Obtained results are presented in Table 2 and show a good agreement with the results from [6].

Table 2. Comparison of C_D values.

C_D	$Re = 10$	$Re = 20$	$Re = 40$
From [6]	2.846	2.045	1.522
LBS	2.437	2.051	1.526

The plot of u_x/U_0 at $Re = 10$ is presented in fig. 4. As it can be seen, obtained results demonstrated a good agreement with the results of R. Mei and W. Shyy obtained in [23] with the usage of bounce-back BC. The small deviations of the plots at this value of Re in contrast to the lid-driven cavity flow can be explained by small value of r_0 in comparison with the linear size of the whole domain ($2R$).

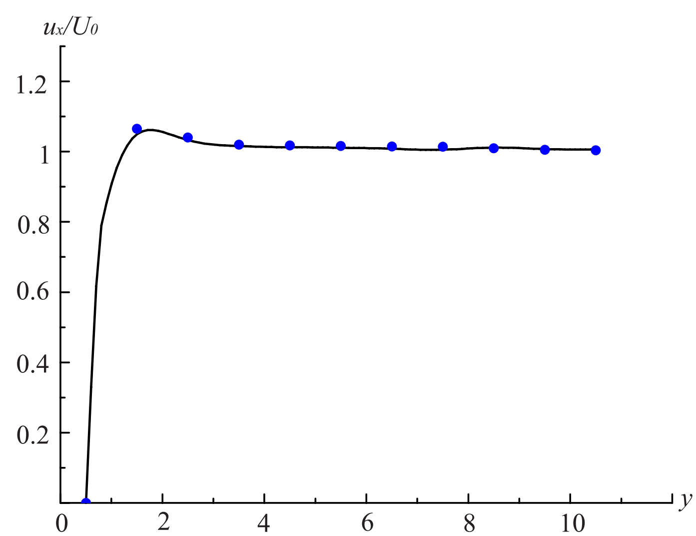

Fig 4. Plot of u_x/U_0 at $Re = 10$. Black line — result obtained by LBS, dots — result from [23]

5 Summary

The finite-element-based LBS for the computations on unstructured meshes is proposed. The scheme is based on the weighted residuals method with Galerkin approximation. The scheme can be classified as semi-implicit in time and is reduced to the solution of the linear algebraic system at every time step.

The investigation of the EBC application showed that usage of this BC type can produced a results which are in good agreement with the results obtained from the solution of hydrodynamical equations at $Re \geq 20$. Favorable results obtained by proposed LBS indicate that the scheme is potentially capable for the computations of viscous flows in complex geometries.

It must be noted, that the proposed scheme can be applied for computations at arbitrary lattices and for computations of three-dimensional flows. Also, the scheme can be applied to the problems for Boltzmann equation with discrete velocities for the case of complex collision term [15].

References

[1] T. Abe, Derivation of the lattice Boltzmann method by means of the discrete ordinate method for the Boltzmann equation, *Journal of Computational Physics,* **131, N. 1** (1997), 241-246.

[2] P. L. Bhatnagar, E. P. Gross, M. Krook, A model for collision processes in gases. I. Small amplitude processes in charged and neutral one-component systems, *Physical Review,* **94, N. 3** (1954), 511 - 525.

[3] J. E. Broadwell, Study of rarefied shear flow by the discrete velocity method, *Journal of Fluid Mechanics,* **19** (1964), 401 - 414.

[4] S. Chen, G. D. Doolen, Lattice Boltzmann method for fluid flows, *Annual Review of Fluid Mechanics,* **30** (1998), 329 - 364.

[5] B. Crouse, E. Rank, M. Kraczyk, J. Tolke, A LB-based approach for adaptive flow simulations, *International Journal of Modern Physics B,* **17, N. 1-2** (2003), 109 - 112.

[6] S. C. R. Dennis, G.-Z. Chang, Numerical solutions for steady flow past a circular cylinder at Reynolds numbers up to 100, *Journal of Fluid Mechanics,* **42, N. 3** (1970), 471 - 489.

[7] G. Eitel-Amor, M. Meinke, W. Schroder, A lattice-Boltzmann method with hierarchically refined meshes, *Computers and Fluids,* **75** (2013), 127 - 139.

[8] O. Filippova, D. Hanel, Grid refinement for lattice-BGK models, *Journal of Computational Physics,* **147** (1998), 219 - 228.

[9] O. Filippova, D. Hanel, Boundary-fitting and local grid refinement for lattice-BGK models, *International Journal of Modern Physics C,* **9, N. 8** (1998), 1271 - 1279.

[10] O. Filippova, D. Hanel, Acceleration of lattice-BGK schemes with grid refinement, *Journal of Computational Physics,* **165** (2000), 407 - 427.

[11] C. Fletcher, *Computational techniques for fluid dynamics,* Springer, Berlin, 1991

[12] S. Foroughi, S. Janshidi, M. Masihi, Lattice Boltzmann method on quadtree grids for simulating fluid flow through porous media: a new automatic algorithm, *Physica A,* **392** (2013), 4772 - 4786.

[13] `http://www.freefem.org`.

[14] U. Ghia, K. N. Ghia, K. N. Shin, High–Re solutions for incompressible flow using the Navier — Stokes equations and multigrid method, *Journal of Computational Physics,* **48** (1982), 387 - 411.

[15] B. I. Green, P. Vedula, A lattice based solution of the collisional Boltzmann equation with applications to microchannel flows, *Journal of Statistical Mechanics: Theory and Experiment,* **7** (2013), 1 - 22.

[16] X. He, L.-S. Luo, A priori derivation of the lattice Boltzmann equation, *Physical Review E,* **55, N. 6** (1997), R6333 - R6336.

[17] T. J. R. Hughes, G. Scovazzi, T. E. Tezduyar, Stabilized methods for compressible flows, *Journal of Scientific Computing,* **43** (2010), 343 - 368.

[18] J. J. Konnor, C. A. Brebbia, *Finite element techniques for fluid flow,* London/Boston, Newnes-Butterworth, 1976.

[19] A. L. Kupershtokh, A lattice Boltzmann equation method for real fluids with the equation of state known in tabular form only in regions of liquid and vapor phases, *Computers and Mathematics with Applications,* **61, N. 12** (2011), 3537-3548.

[20] A. L. Kupershtokh, Three-dimensional LBE simulations of a decay of liquid dielectrics with a solute gas into the system of gas-vapor channels under the action of strong electric fields, *Computers and Mathematics with Applications,* **67, N. 2** (2014), 340-349.

[21] J. Latt, B. Chopard, O. Malaspinas, M. Deville, A. Michler, Straight velocity boundaries in the lattice Boltzmann method, *Physical Review E,* **77** (2008), 056703-1 - 056703-16.

[22] T. Lee, C.-L. Lin, A characteristic Galerkin method for discrete Boltzmann equation, *Journal of Computational Physics,* **171** (2001), 336 - 356.

[23] R. Mei, W. Shyy, On the finite difference–based lattice Boltzmann method in curvilinear coordinates, *Journal of Computational Physics,* **143** (1998), 426 - 448.

[24] M. Mirzaci, A. Poozech, Simulation of fluid-flow in a body-fitted grid system using the lattice Boltzmann method, *Physical Review E,* **87** (2013), 063312-1 - 063312-9.

[25] A. A. Mohamad, S. Succi, A note on equilibrium boundary conditions in lattice Boltzmann fluid dynamic simulations, *The European Physical Journal Special Topics,* **171** (2009), 213 - 221.

[26] R. R. Nourgaliev, T. N. Dinh, T. G. Theofanous, D. Joseph, The lattice Boltzmann equation method: theoretical interpretation, numerics and implications, *International Journal of Multiphase Flow,* **29** (2003), 117 - 169.

[27] C. Pan, L. S. Luo, C. T. Miller, An evaluation of lattice Boltzmann schemes for porous medium flow simulation, *Computers and Fluids,* **35** (2006), 898 - 909.

[28] D. V. Patil, K. N. Lakshmisha, Two-dimensional flow past circular cylinders using finite volume lattice Boltzmann formulation, *International Journal for Numerical Methods in Fluids,* **69** (2012), 1149 - 1164.

[29] G. Peng, H. Xi, C. Duncan, S.-H. Chou, Lattice Boltzmann method on irregular meshes, *Physical Review E,* **58, N. 4** (1998), R4124 - R4127.

[30] G. Peng, H. Xi, C. Duncan, S.-H. Chou, Finite volume scheme for the lattice Boltzmann method on unstructured meshes, *Physical Review E,* **59, N. 4** (1999), 4675 - 4682.

[31] G. Peng, H. Xi, S.-H. Chen, On boundary conditions in the finite volume lattice Boltzmann method on unstructured meshes, *International Journal of Modern Physics C,* **10, N. 6** (1999), 1003 - 1016.

[32] P. R. Rinaldi, E. A. Dari, M. J. Venere, A. Clansse, A lattice Boltzmann solver for 3D fluid simulation on GPU, *Simulation Modelling Practice and Theory,* **25** (2012), 163 - 171.

[33] M. Schreiber, P. Neumann, S. Zimmer, H. J. Bungartza, Free-surface lattice-Boltzmann simulation on many-core architectures, *Procedia Computer Science,* **4** (2011), 984 - 993.

[34] M. Seino, T. Tanahashi, K. Yasuoka, An analysis of natural convection using the thermal finite element discrete Boltzmann equation, *Computers and Fluids,* **40, N. 1** (2010), 113 - 117.

[35] X. Shan, H. Chen, Lattice Boltzmann model for simulating flows with multiple phases and components, *Physical Review E,* **47** (1993), 1815 - 1819.

[36] V. Sofonea, A. Lamura, G. Gonnella, A. Cristea, Finite-difference lattice Boltzmann model with flux limiters for liquid-vapor systems, *Physical Review E,* **70** (2004), 046702-1 - 046702-9.

[37] V. Sofonea, R. F. Sekerka, Viscosity of finite difference lattice Boltzmann models, *Journal of Computational Physics,* **183** (2003), 422 - 434.

[38] J. D. Tritton, Experiments on the flow past a circular cylinder at low Reynolds numbers, *Journal of Fluid Mechanics,* **6** (1959), 547 - 567.

[39] S. Ubertini, S. Succi, A generalised lattice Boltzmann equation on unstructured grids, *Communications in Computational Physics,* **3, N. 2** (2008), 342 - 356.

[40] S. Ubertini, G. Bella, S. Succi, Lattice Boltzmann method on unstructured grids: further developments, *Physical Review E,* **68** (2003), 016701 - 1-016701-10.

[41] S. Ubertini, S. Succi, G. Bella, Lattice Boltzmann schemes without coordinates, *Philosophical Transactions of the Royal Society A,* **362, N. 1821** (2004), 1763 - 1771.

[42] J. C. G. Verschaeve, Analysis of the lattice Boltzmann Bhatnagar–Gross–Krook no-slip boundary condition: ways to improve accuracy and stability, *Physical Review E,* **80** (2009), 036703-1 - 056703-23.

[43] K. E. Wardle, T. Lee, Finite element lattice Boltzmann simulations of free surface flow in a concentric cylinder, *Computers and Mathematics with Applications,* **65** (2013), 230 - 238.

[44] F. Weichert, C. Mertens, L. Walczak, G. Kern–Isberner, M. Wagrer, A novel approach for connecting temporal-ontologies with blood flow simulations, *Journal of Biomedical Informatics,* **46** (2013), 470 - 479.

[45] D. A. Wolf-Gladrow, *Lattice-gas cellular automata and lattice Boltzmann models — an introduction,* Springer-Verlag, Berlin, 2005.

[46] J. Wu, C. Shu, A solution-adaptive lattice Boltzmann method for two-dimensional incompressible viscous flow, *Journal of Computational Physics,* **230** (2011), 2246 - 2269.

[47] H. Xi, G. Peng, S.-H. Chou, Finite-volume lattice Boltzmann method, *Physical Review E,* **59, N. 5** (1999), 6202 - 6205.

[48] H. Xi, G. Peng, S.-H. Chou, Finite-volume lattice Boltzmann schemes on two and three dimensions, *Physical Review E,* **60, N. 3** (1999), 3380 - 3388.

[49] Q. G. Xiong, B. Li, J. Xu, X. J. Fang, X. W. Wang, L. M. Wang, X. F. He, W. Ge, Efficient parallel implementation of the lattice Boltzmann method on large clusters of graphic processing units, *Computer Science and Technology,* **57, N. 7** (2012), 707 - 715.

[50] A. Zarghami, M. J. Maghrebi, S. Ubertini, S. Succi, Modeling of bifurcation phenomena in suddenly expanded flows with a new finite volume lattice Boltzmann method, *International Journal of Modern Physics C,* **22, N. 9** (2011), 977 - 1003.

[51] J. Zhang, Effect of suspending viscosity on red blood cell dynamics and blood flows in microvessels, *Microcirculation,* **18** (2011), 562 - 573.

[52] Z. Zhao, P. Huang, Y. Li, J. Li, A lattice Boltzmann method for viscous free surface waves in two dimensions, *International Journal for Numerical Methods in Fluids,* **71** (2013), 223 - 248.

Received: January 15, 2014